Journal of Peptide Science
J. Pept. Sci. 2008; **14**: 1173–1182
Published online 6 August 2008 in Wiley InterScience (www.interscience.wiley.com). DOI: 10.1002/psc.1055

JOURNAL OF PEPTIDE SCIENCE

Molecular dynamic simulations of nanomechanic chaperone peptide and effects of *in silico* His mutations on nanostructured function

ABOLFAZL BARZEGAR,[a,b] ALI AKBAR MOOSAVI-MOVAHEDI,[a,c]* KARIM MAHNAM,[a] HOMAYOON BAHRAMI[a] and NADER SHEIBANI[d]

[a] Institute of Biochemistry and Biophysics, University of Tehran, Tehran, Iran
[b] Research Institute of Fundamental Sciences, University of Tabriz, Tabriz, Iran
[c] Foundation for Advancement of Science and Technology in Iran (FAST-IR), Tehran, Iran
[d] Department of Ophthalmology and Visual Sciences, University of Wisconsin School of Medicine and Public Health, Madison, WI, USA

Received 25 March 2008; Revised 11 May 2008; Accepted 26 May 2008

Abstract: The nanoscale peptide YSGVCHTDLHAWHGDWPLPVK exhibits molecular chaperone activity and prevents protein aggregation under chemical and/or thermal stress. Here, His mutations of this peptide and their impact on chaperone activity were evaluated using theoretical techniques. Molecular dynamic (MD) simulations with simulated annealing (SA) of different mutant nanopeptides were employed to determine the contribution of the scaffolding His residues (H45, H49, H52), when mutated to Pro, on chaperone action *in vitro*. The *in silico* mutations of His residues to Pro (H45P, H49P, H52P) revealed loss of secondary ordered strand structure. However, a small part of the strand conformation was formed in the middle region of the native chaperone peptide. The His-to-Pro mutations resulted in decreased gyration radius (R_g) values and surface accessibility of the mutant peptides under the simulation times. The invariant dihedral angle (ϕ) values and the disrupting effects of the Pro residues indicated the coil conformation of mutant peptides. The failure of the chaperone-like action in the Pro mutant peptides was consistent with their decreased effective accessible surfaces. The high variation of Φ value for His residues in native chaperone peptide leads to high flexibility, such as a minichaperone acting as a nanomachine at the molecular level. Our findings demonstrate that the peptide strand conformation motif with high flexibility at nanoscale is critical for chaperone activity.

Keywords: chaperone; nanomachine; aggregation; *in silico* mutation; simulation; molecular dynamics

INTRODUCTION

It is estimated that more than half of human diseases are caused by protein-folding defects [1]. Chaperones provide considerable protection against diseases associated with protein misfolding and aggregation [2–5]. They act as stable complexes with the partially unfolded and/or misfolded proteins preventing aggregation and restoring known folding machines [6]. Critical residues are required for the chaperone-like function of most chaperones, including the small heat-shock protein (sHSP) α-crystallin [7] and oligomeric GroEL chaperone [8]. The monomeric apical domain of GroEL (residues 191–345), referred to as 'minichaperone', exhibits a GroEL-like activity [8]. The residues 57–69 and 93–107 of α-crystallin are significant parts of the protein that affect chaperone action and are known as 'chaperone-function peptides' [9]. The chaperone-function peptides in α-crystallin have a function similar to the whole α-crystallin protein. That is, they possess the antiaggregation property, even in isolation from the native α-crystallin protein [7]. These peptides have a special appeal owing to their chemical diversity, richness of shapes, relative chemical and physical stability, their simple structure, the possibility of being synthesized in large quantity, the most favorable building blocks for the design, and synthesis of nanostructures and their use in bionanotechnology [10].

A 21-amino-acid peptide from the yeast alcohol dehydrogenase (ADH) is the binding site for α-crystallin [11]. This 21-amino-acid peptide (YSGVCHTDLHAWHGDWPLPVK) exhibits a chaperone-like activity as a minichaperone. It represents the middle region (residues 40–60) of the yeast ADH, known as *the unique region*. Like all other sHSPs, this peptide is referred to as an 'intramolecular chaperone', which forms stable complexes with a wide variety of chemically or thermally denatured proteins [12]. The mutation of each of the three His residues to Pro (H45P, H49P, H52P) results in loss of chaperone-like activity of the peptide [12]. However, it is generally believed that the chaperone proteins display high amounts of Pro residues in their primary structure [13,14]. Unfortunately it is not easy to experimentally define the mechanisms and reasons for lack of chaperone activity of the His-mutated peptides. Understanding the physicochemical determinants that underlie peptide action as nanomachine in

*Correspondence to: Ali Akbar Moosavi-Movahedi, Institute of Biochemistry and Biophysics, University of Tehran, Tehran, Iran;
e-mail: moosavi@ibb.ut.ac.ir

chaperone activity (preventing aggregation), are fundamental in the rational design of nanostructures for new drugs, which are able to interfere with the harmful aggregated amyloid-formation process.

The combined efforts of experimental and theoretical approaches have been useful in expanding our understanding of the physicochemical properties of peptides. Molecular dynamic (MD) simulations have been used to faithfully estimate the physical properties of various peptides, which are not accessible to direct experimental observations [15–18]. MD simulation is an important tool to understand not only the effect of mutations on the structure, but also more importantly, the dynamic nature of the protein molecules [18–20]. It has been widely used for the investigation of aggregation at the molecular level [21–24]. Furthermore, the *in silico* mutation analysis can provide useful information regarding the secondary and tertiary conformation of macromolecules, especially the functional mechanisms contributed by the striking residues in the primary structure [25,26].

The mechanism of the GroEL chaperone action was recently studied using MD simulation [27]. In addition, the simulation has been used to evaluate peptide folding in solution under reversible conditions at atomic resolution, and to test the models of the folding process [28,29]. Here, the chaperone inability of the mutant nanomachine ADH minichaperone peptides were investigated by MD simulations in order to gain further insight into the mechanisms and the biophysical properties of vital residues in secondary and tertiary structures. Thus, theoretical modeling may provide insight into the design of more effective nanoscale minichaperone peptides.

Computational Schemes

All simulations were performed using the GROMACS simulation package [30,31]. The time step of integration was held at 1fs with the G43a1 force field [29] in these simulations. To demonstrate the quality of the simulation data, the root-mean-square deviations (RMSD) of the simulated molecular systems were determined by averaging the overtime intervals of 50 ps. Additional details regarding the MD simulations are described in the following sections.

Theoretical Procedures

Here we determined the effects of *in silico* His mutations on the ADH chaperone peptide function using MD simulations. The equilibrium geometries of the ADH peptide (ten different samples) at 300 K were first achieved using MD simulation. The lowest energy of equilibrium structure was then employed to design the initial configuration of the mutant peptides. MD simulations were employed to evaluate the mutation effects and to obtain 30 different equilibrium geometries. The local minima geometries (40 geometries) for all species were then obtained using the annealing simulation and molecular mechanics (MM) minimization methods. The calculation details are indicated in the subsequent sections.

Molecular Dynamic Simulations

The initial configuration of the ADH peptide YSGVCHTDLHAWHGDWPLPVK was taken from the 2HCY PDB code. To remove the effects of the long-range strains, which may impact conformations in the intermolecular X-ray coordinates, we performed a simulated study of the ADH peptide for 10 ns. MD simulations were carried out at NPT ensemble and periodic boundary conditions. The electrostatic interactions were calculated using the Particle Mesh Ewald model [32] with a 14 Å cutoff. The ADH X-ray structure was placed in a solvent box with approximately 3000 SPC 216 water molecules. The distance from the cubic-box edges of the chaperone peptide was 7 Å. The neutralization of the system required the addition of 1 Na^+ ion.

The aqueous solvent and the Na^+ ions were first subjected to the energy minimization with solute kept fixed in its initial configuration. The solvent and the Na^+ ions were then allowed to evolve using an MD simulation for 20 ps with a step time of 1 fs, keeping the structure of the solute molecule fixed. The entire system was then minimized using the steepest descent of 1000 steps followed by the conjugate gradients of 9000 steps. In order to obtain an equilibrium geometry at 300 K and 1 atm, the system was heated at a weak temperature (0.1 K) and pressure (0.5 atm), and took advantage of the Berendesen algorithms [33]. The heating time for the MD simulations at 100, 200, and 300 K was 100 ps. An MD simulation was then conducted for 10 000 ps and ten geometries were statistically generated during 9000–10 000 ps (with 100 ps intervals), which were followed by a structural minimization calculation. The latter minimization was performed at the steepest descent of 1000 steps followed by the conjugate gradients of 9000 steps. Finally just the minimum geometry based on calculation of hydration-free energy ($\Delta G_{hydration}$) [34–37] was obtained (from the mentioned ten geometries) for the chaperone peptide.

The selected minimum geometry was employed as a template for generation of the mutant peptides, Mut1–Mut3. The His residues of the ADH peptide were mutated *in silico* to Pro including H45P (Mut1), H49P (Mut2) and H52P (Mut3), respectively. Each of the structures (Mut1–Mut3), which had been proposed as chaperone failure [12], was used as a starting point for the additional 10 ns simulation. Thirty different geometries were generated as indicated above for the native chaperone peptide and only the minimum geometries (Mut1–Mut3) were presented via calculation

DOI: 10.1002/psc

of $\Delta G_{hydration}$. The lowest energies of the 40 different equilibrium geometries generated from MD simulation conformations were obtained by calculating $\Delta G_{hydration}$ for simulated annealing (SA) procedures, described below.

Simulated Annealing Procedures

The heating/annealing cycles facilitate the avoidance of local minima and provide the best solution to the global minimum. The SA MD's full-energy minimization strategy is necessary to enable the molecule to

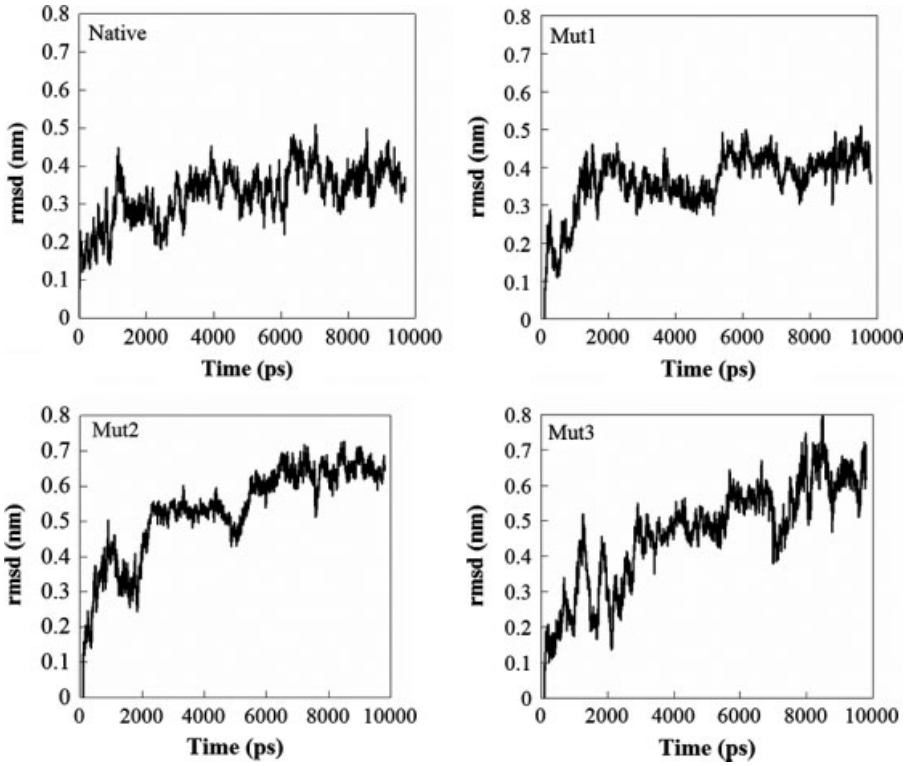

Figure 1 Root-mean-square deviations (RMSDs) of the main-chain atoms (backbone) *versus* simulation time (ps). The native peptide has steady-state conformation after 4000 ps, whereas the mutant peptides (Mut1–Mut3) take steady-state conformation after 6000 ps. There are notable differences in the native and mutant peptides RMSD values.

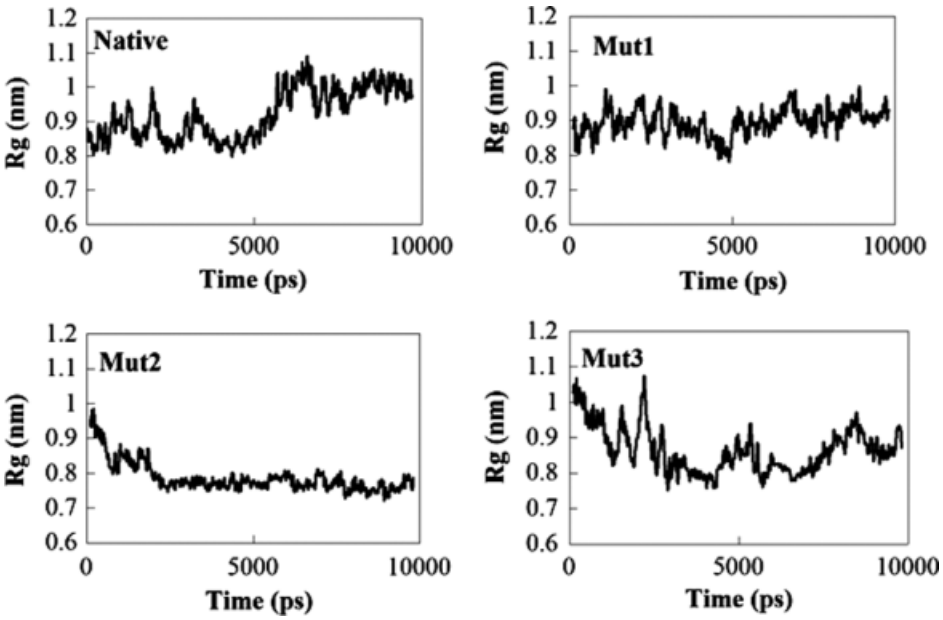

Figure 2 The R_g values for the native chaperone and mutant peptides during simulation times. Symbols (Mut1–Mut3) indicate the H6P, H10P and H13P mutant peptides, respectively.

DOI: 10.1002/psc

overcome energy barriers [38,39] between different conformations, and to prevent the system from getting stuck in a particular region of the conformational space. Thus, SA method was employed to obtain more local minimized geometries of each species and conformational sampling of each equilibrium geometry at 300 K.

The minimum structure from the MD geometries of the native and mutant chaperone peptides were used for SA calculations. Each of the indicated structures was placed in the solvent box, as previously described. In this SA method, heating treatment up to 1000 K was first performed on the four systems with a 50 ps duration, keeping all parameters the same as before. This was then followed by the annealing treatment on these systems. The strategy, being decreased in temperature from 1000 to 50 K, was followed by an increase from 50 to 1000 K. The time duration for each increase or decrease in temperature was 100 ps. Performing in this manner, the SA of 2 ns resulted in 40 near-local minima structures (ten structures for each starting system). The inspection of the annealed systems showed no indication of any bond breakage or tension in the structures as expected. Thus, the use of temperatures as high as 1000 K did not have any effect on the destruction of the aforementioned structures. In order to obtain local minima structures, the annealed geometries were then optimized by taking advantage of the steepest descent of 1000 steps (down to a gradient of $<$100 kJ/mol/nm) followed by the conjugate gradients of 9000 steps (down to a gradient of $<$10 kJ/mol/nm). Finally four minimum geometries from the 40 generated structures of the native and mutant (Mut1–Mut3) peptides were presented based on the calculation of $\Delta G_{\text{hydration}}$.

RESULTS

Coordination of Extracted Chaperone Peptide

The analysis of the secondary ordered conformation of the native chaperone peptide is shown in Table 1 (first line). The results indicated that the first four residues, from the free initial chaperone peptide that was directly extracted of 2HCY PDBexhibitstrand coordinates. The next seven residues were related to the helix conformation, while the remaining ten residues participated in the random coil. However, this coordination was related to the state that was induced by excessive strain on the ADH protein. The real conformation of this peptide in the free state should be different from the starting structure directly extracted from 2HCY PDB. Thus MD simulation was utilized to remove excessive strains and generate a well-defined peptide structure.

Table 1 Secondary structure of the chaperone peptides directly taken from the PDB 2HCY (native X-ray) and after 10 000 ps simulation of native and mutant peptides. The symbols 's', 'h', and 'l' indicate the contribution to the strand of each of the residues of helix and loop (coil) secondary structures in the related peptides, respectively. The residues 1–21 correspond to the amino acids 40–60 of the yeast ADH

Amino-acid sequence	Y	S	G	V	C	H	T	D	L	H	A	W	H	G	D	W	P	L	P	V	K
	1	2	3	4	5	6	7	8	9	10	11	12	13	14	15	16	17	18	19	20	21
Native X-ray	s	s	s	s	l	l	h	h	h	h	h	h	h	l	l	l	l	l	l	l	l
Native simulated	l	l	l	l	l	l	h	h	h	h	h	h	l	l	l	l	l	l	l	l	l
Mut1 simulated	l	l	l	l	l	l	h	h	h	l	l	l	l	l	l	l	l	l	l	l	l
Mut2 simulated	l	l	l	l	l	l	h	h	h	h	l	l	l	l	l	l	l	l	l	l	l
Mut3 simulated	l	l	l	l	l	l	h	h	h	l	l	l	l	l	l	l	l	l	l	l	l

Table 2 Prediction of the secondary structure of the chaperone peptides with the PROF program [40]. The sequences indicated below are related to the native and mutant peptide residues. The symbol, 'l' indicates each of the residues contributing to the loop (coil) secondary structure. Blank cells denote the inability of PROF program to predict structure. The residues 1–21 correspond to the amino acids 40–60 of the yeast ADH

Amino-acid sequence	Y	S	G	V	C	H	T	D	L	H	A	W	H	G	D	W	P	L	P	V	K
	1	2	3	4	5	6	7	8	9	10	11	12	13	14	15	16	17	18	19	20	21
PROF secondary prediction (native)	l	l	—	—	—	—	l	—	—	—	—	—	—	l	l	l	l	l	l	l	l
PROF secondary prediction (Mut1)	l	l	—	—	—	l	l	l	—	—	—	—	—	l	l	l	l	l	l	l	l
PROF secondary prediction (Mut2)	l	l	—	—	—	l	l	l	l	l	l	—	l	l	l	l	l	l	l	l	l
PROF secondary prediction (Mut3)	l	l	—	—	—	—	l	l	l	l	l	l	l	l	l	l	l	l	l	l	l

DOI: 10.1002/psc

MD Simulation of Native and Mutant Chaperone Peptides

Due to PDB deficiency of the 21-amino-acid ADH chaperone peptide, we extracted its initial coordinates from the PDB structure of the 2HCY. MD simulation method was then applied, which allowed approaching the native form of the free peptide and stabilization of the structure. Figure 1 shows the RMSDs of the native and mutant chaperone peptide backbones under MD simulation times. After a 4000 ps simulation, the RMSDs of the native conformation were kept at 0.4 nm for 6000 ps, indicating that after elimination of the unfavorable long-range forces from the X-ray geometry the chaperone peptide acquired a rather stable form. Considering conformational sampling from final MD simulation conformers showed almost all peptides (native and Mut1–Mut3) tend to loose their ordered nanostructure (especially strand) to coil coordinates (Table 1). The tendency to lose ordered conformation among mutant peptides was more predominant than the native peptide.

Assessments of Gyration Radius (R_g) during Simulation Times

Changing gyration radius (R_g) of all peptides *versus* simulation time agreed with RMSDs values further supporting the validity and sufficiency of 10 000 ps MD simulation time with the quality of the simulation data (Figure 2). Assaying R_g, which was the criterion of the tertiary structural volume, indicated that the His-to-Pro mutations caused a decrease in R_g values under the simulation times. After averaging the R_g values in the final 3000 ps of the simulation time (steady-state conformation population) the R_g values in the range of nanoscale were obtained for each peptide (Figure 3). Figure 3 illustrates the role of Pro in decreased tertiary structural volume. Figures 2 and 3 show that the mutations of His residues resulted in decreased R_g values and surface accessibility. The tertiary structure of the peptides, based on stick style, is shown in Figure 4. The disruption property of the Pro mutant peptides, due to loss of ordered conformation, resulted in lower R_g values in these peptides.

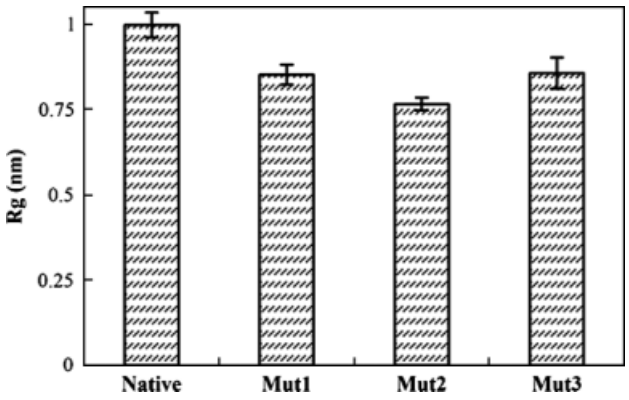

Figure 3 The average R_g values for the native chaperone and mutant peptides during the final 3000 ps simulation time. Symbols (Mut1–Mut3) indicate the H6P, H10P, and H13P mutant peptides, respectively.

Coordination of Native and Mutant Chaperone Peptides by PROF Program

The results from the application of PROF program are summarized in Table 2. These results indicate that each mutant peptide illustrated a greater coil conformation than the native peptide, which confirms aforementioned MD simulation data. The PROF program is very simple and can predict protein structure with more than 70% accuracy [40].

Acquiring the Real Peptide Conformation by SA

The native state of a protein is generally believed to be a global free-energy minimum. Thus, the SA technique is a powerful method for acquiring the real peptide conformation [38,39]. The SA results, only the lowest energy structure of each conformation, are presented in Table 3. These results show that Pro mutations promoted the entire random coil structure of the chaperone peptides. However, in the structure of the native peptide a small part of the strand conformation was observed in the middle region due to the presence

Table 3 Secondary structure of the native and the mutated chaperone ADH peptides, which were simulated annealed. The symbol 's', 'h' and 'l' indicate each residue contribution to the strand, helix and loop (coil) secondary structure in the related peptides. The residues 1–21 correspond to the amino acids 40–60 of the yeast ADH

Amino-acid sequence	Y	S	G	V	C	H	T	D	L	H	A	W	H	G	D	W	P	L	P	V	K
	1	2	3	4	5	6	7	8	9	10	11	12	13	14	15	16	17	18	19	20	21
Native	l	l	l	l	l	s	s	s	s	s	s	s	l	l	l	l	l	l	l	l	l
Mut1	l	l	l	l	l	l	l	l	l	l	l	l	l	l	l	l	l	l	l	l	l
Mut2	l	l	l	l	l	l	l	l	l	l	l	l	l	l	l	l	l	l	l	l	l
Mut3	l	l	l	l	l	l	l	l	l	l	l	l	l	l	l	l	l	l	l	l	l

DOI: 10.1002/psc

of His residues. Figure 5 depicts the superposition stick-style tertiary structure of the native and mutant peptides determined by SA, which are related to the collapsed conformations of Pro mutant peptides.

Evaluation of Dihedral Angles (ϕ) during MD Simulation

Figure 6 shows that the dihedral angles (ϕ) of the Pro residues are stable, remaining within a small range throughout the whole simulation time. In contrast, the dihedral angle ϕ related to the His residues varied considerably. This high variation and flexibility provided His residues the possibility of interacting with other residues forming suitable secondary structures, such as a strand.

DISCUSSION

The MD simulations of peptide stability and folding are currently an area of intense activity. The computational studies of helix and sheet-forming peptides are reliably used to assess physicochemical properties of various peptides [28,29,41–58]. The MD simulations, starting from a fully extended random conformation of the peptide (all backbone dihedral angles in *trans*), were recently performed at different temperatures to study peptide folding [28,29]. If a region of the molecule is highly strained the MD simulation attempts to release the strain leading to a native conformation, which is possible to evaluate by changes in RMSDs. Here, variations in RMSDs of the mutant peptides were greater than native peptide during MD simulation times. The RMSDs of the mutant peptides increased within 6000 ps and then fluctuated in nanoscale about 0.5–0.6 nm. The large RMSDs of the mutant peptides were due to drastic structural changes in the initial conformation of the mutant peptides. Evaluation of R_g values confirmed that more conformational changes occurred in the mutant peptides. The native peptide with 1 nm R_g value has high chaperon action and operates as a nanomachine *in vitro*, whereas mutant peptides (Mut1–Mut3) with lower R_g values lacked any chaperone potency. In addition, the results from MD

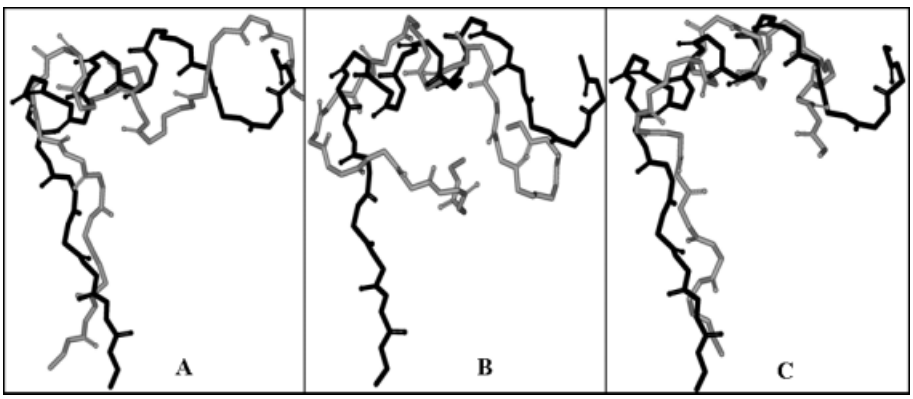

Figure 4 Simulated stick-style tertiary structures of native and mutant peptides. Images of simulated peptides were generated with DS Viewer Pro. In all panels, dark stick lines denote native peptide structure, and gray stick lines in A, B and C panels, denote mutant (Mut1–Mut3) peptide conformations, respectively. During 9000–10 000 ps MD simulations, statistically ten geometries from each peptide were generated as a conformational sampling, and only the lowest energy structure of each conformation is shown.

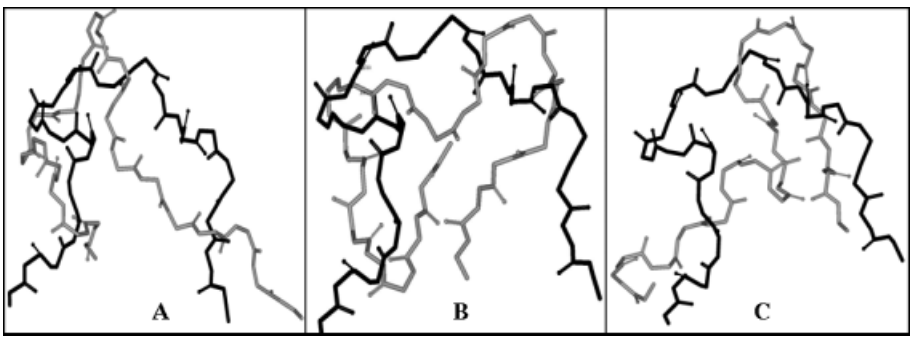

Figure 5 Simulated annealing (SA) stick-style tertiary structures of native and mutant peptides. Images of SA peptides were generated with DS Viewer Pro. In all panels, dark stick lines denote native peptide structure, and gray scales lines in A, B and C panels denote mutant peptides structure (Mut1–Mut3) respectively. Only the lowest energy structure from the ten sampling geometry of each conformation is shown.

DOI: 10.1002/psc

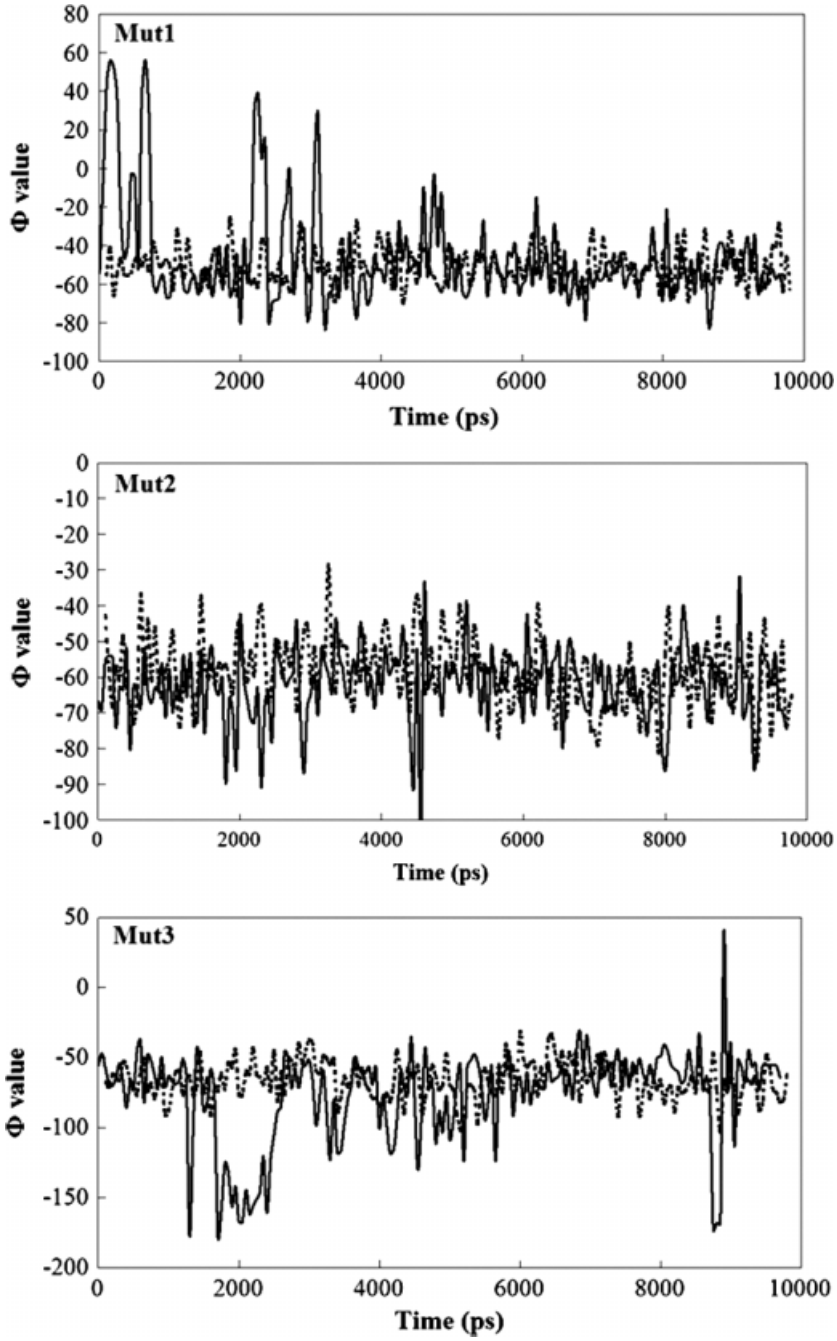

Figure 6 ϕ distribution for the Pro and His residues during simulation. Filled and dashed lines denote ϕ values of His and Pro mutant peptides during the simulation time, respectively. Symbols (Mut1–Mut3) indicate the H6P, H10P and H13P peptides, respectively.

simulation and PROF program predictions illustrate that the His mutations resulted in decreased secondary ordered helix conformation that was accompanied by an increased coil conformation (Tables 1 and 2). Pro is an unusual amino acid (imino acid), and replacing the His residues with Pro disrupts the peptide structure leading to decreased R_g values and surface accessibility. The chaperone action involves interactions with target protein and protein complex formation [6]. Furthermore, the effective-surface accessibility is important for the construction of a stable substrate protein-chaperone complex and prevention of aggregation.

Both MD and PROF program studies suggested that the peptides in the mutant form tend to form a random coil structure. That is, the simulated native and mutant peptides lose most of their secondary ordered structures during the 10 000 ps simulation time exhibiting a tendency for conformational transition. The tendency to form coil conformation in mutant peptides (Mut1–Mut3), by eliminating the local barrier energy

DOI: 10.1002/psc

via SA method, confirmed the aforementioned results. However, the native peptide has a propensity to form a small part of strand conformation in the middle region. The results of SA method are more reliable and it is believed that by eliminating the local barrier energy one can approach the real conformation. Our data are in agreement with the experimental CD results showing that all the mutant peptides exhibit a greater extent of random coil structure compared with native ADH peptide [12]. However, the CD spectropolarimetry provides data that only approximates the secondary structure of macromolecules. In contrast, NMR, X-ray crystallography, and the theoretical methods are able to elucidate structures in more details. In this context, theoretical results indicated the vital role of seven residues that construct ordered strand nanostructure conformation in the native nanoscale chaperone peptide.

Another physical parameter that explains the reason for the collapse of tertiary structure of mutant peptides is constancy of thedihedral angle ϕ. The mutation of Pro to Leu in prion protein results in an increase in the variation of the dihedral angle ϕ promoting the β-sheet construction. Thus, Pro is critical in preventing the transition from random to the β-sheet structure [18]. Therefore, the invariant Φ value can demonstrate the disrupting effects of Pro residues leading to the random coil conformation of the mutant peptides. The high variation of the Φ value for His residues in the ADH chaperone peptide could lead to higher flexibility of the native peptide, such as minichaperone action. However, the flexibility of the mutant peptides was lower because of constant Φ values. Thus, the native chaperone nanopeptide could easily interact with aggregation prone state macromolecules, while the mutant peptides could not. Furthermore, it appears that the strand section of the peptide in its native state consists of the major part for the chaperone-like activity of the peptide. These theoretical findings agree with a previous report regarding the substitution of the Phe residues with Gly in the chaperone 19-amino acid peptide from the α-crystallin. The substitutions caused a 20-fold decrease in chaperone action and the mutated peptide did not show a secondary structure. The α-crystallin, as a small heat shock chaperone protein, has a considerable secondary structure [12]. These findings demonstrate that Pro mutations were conflicting with the secondary ordered conformation. Mutation of each of the His residues to Pro caused the loss of its crucial strand nanostructure and led to coil structure with low surface accessible area in the tertiary conformation resulting in lack of chaperone action.

The chaperone proteins interact with the aggregation-prone state of macromolecules. These interactions mask the aggregation surfaces and culminate in antiaggregation effects. The loss of secondary ordered structure with the collapsing tertiary conformation, and decreased effective-surface accessibility of the Pro mutant chaperone peptides, caused failure in antiaggregation activity. Thus, the strand conformation of the peptide is critical for its chaperone activity, and the His mutation to Pro leads to disruption of this region. These calculations establish a link between sequences and nanostructured conformation of nanopeptides with antiaggregation propensities and suggest that special residues may be targeted in new minichaperones for drug design. On the basis of this finding we propose the reliable model to design new sequences with selected properties for nanobiotechnological applications.

CONCLUSIONS

Theoretical techniques are presently a reasonable alternative for atomic-resolution investigation of many complex processes, despite recent progresses in the development of experimental analysis techniques. The *in vitro* mutations of minichaperone (21 amino acid) H45P (Mut1), H49P (Mut2) and H52P (Mut3) illustrated the failure action of this peptide as a nanomachine. In order to determine the main factor(s) that contribute to the chaperone activity, we used MD simulation for 10 ns followed by SA of 2 ns. Our results show that the ordered secondary strand nanostructure with seven residues is critical for the chaperone activity of the peptide. The replacement of the histidine residues with proline (a structure-disrupting amino acid) prevented the transition from random structure to secondary ordered structure. This was associated with a fixed dihedral angle ϕ leading to the disruption of tertiary conformation and failure in chaperone action. These findings provide additional insight into physicochemical and functional properties of chaperone systems on the nanoscale. In addition, this knowledge can be exploited for the development of new minichaperones with ordered atomistic structure and rationally designed nanostructures with potentially important applications in biotechnology, molecular medicine, and drug delivery.

Acknowledgements

Financial support from the Research Council of the University of Tehran, as well as the Iran National Foundation of Science (INSF), are gratefully acknowledged.

REFERENCES

1. Fisher MT. Proline to the rescue. *Proc. Natl. Acad. Sci. U.S.A.* 2006; **103**: 13265–13266.
2. Hendrick JP, Hartl FU. Molecular chaperone functions of heat-shock proteins. *Annu. Rev. Biochem.* 1993; **62**: 349–384.
3. Kelley WL, Georgopoulos C. Chaperones and protein folding. *Curr. Opin. Cell Biol.* 1992; **4**: 984–991.

4. Cohen FE. Protein misfolding and prion diseases. *J. Mol. Biol.* 1999; **293**: 313–320.
5. Bellotti V, Mangione P, Stoppini M. Biological activity and pathological implications of misfolded proteins. *Cell. Mol. Life Sci.* 1999; **55**: 977–991.
6. Lee JS, Samejima T, Liao JH, Wu SH, Chiou SH. Physiological role of the association complexes of alpha-crystallin and its substrates on the chaperone activity. *Biochem. Biophys. Res. Commun.* 1998; **244**: 379–383.
7. Sharma KK, Kumar RS, Kumar GS, Quinn PT. Synthesis and characterization of a peptide identified as a functional element in αA-crystallin. *J. Biol. Chem.* 2000; **275**: 3767–3771.
8. Zahn R, Buckle AM, Perrett S, Johnson CM, Corrales FJ, Golbik R, Fersht AR. Chaperone activity and structure of monomeric polypeptide binding domains of GroEL. *Proc. Natl. Acad. Sci. U.S.A.* 1996; **93**: 15024–15029.
9. Sharma KK, Kaur H, Kester K. Functional elements in molecular chaperone alpha crystallin: identification of binding sites in alpha B-crystallin. *Biochem. Biophys. Res. Commun.* 1997; **239**: 217–222.
10. Colombo G, Soto P, Gazit E. Peptide self-assembly at the nano-scale: a challenging target for computational and experimental biotechnology. *Trends Biotechnol.* 2007; **25**: 211–218.
11. Santhoshkumara P, Sharma KK. Identification of a region in alcohol dehydrogenase that binds to α-crystallin during chaperone action. *Biochim. Biophys. Acta* 2002; **1598**: 115–121.
12. Bhattacharyya J, Santhoshkumar P, Sharma KK. A peptide sequence – YSGVCHTDLHAWHGDWPLPVK [40–60] – in yeast alcohol dehydrogenase prevents the aggregation of denatured substrate proteins. *Biochem. Biophys. Res. Commun.* 2003; **307**: 1–7.
13. Guha S, Manna TK, Das KP, Bhattacharyya B. Chaperone-like activity of tubulin. *J. Biol. Chem.* 1998; **273**: 30077–30080.
14. Morgan PE, Treweek TM, Linder RA, Price WE, Carver JA. Casein proteins as molecular chaperones. *J. Agric. Food Chem.* 2005; **53**: 2670–2683.
15. Sekijima M, Motono C, Yamasaki S, Kaneko K, Akiyama Y. Molecular dynamics simulation of dimeric and monomeric forms of human prion protein: insight into dynamics and properties. *Biophys. J.* 2003; **85**: 1176–1185.
16. Lemaitre V, Ali R, Kim CG, Watts A, Fischer WB. Interaction of amiloride and one of its derivatives with Vpu from HIV-1: a molecular dynamics simulation. *FEBS Lett.* 2004; **563**: 75–81.
17. Ivanov AA, Fricks I, Harden TK, Jacobson KA. Molecular dynamics simulation of the P2Y14 receptor Ligand docking and identification of a putative binding site of the distal hexose moiety. *Bioorg. Med. Chem. Lett.* 2007; **17**: 761–766.
18. El-Bastawissy E, Knaggs MH, Gilbert IH. Molecular dynamics simulations of wild-type and point mutation human prion protein at normal and elevated temperature. *J. Mol. Graph. Model.* 2001; **20**: 145–154.
19. Lee H, Kandasamy SK, Larson RG. Molecular dynamics simulations of the anchoring and tilting of the lung-surfactant peptide SP-B1-25 in palmitic acid monolayers. *Biophys. J.* 2005; **89**: 3807–3821.
20. Okimoto N, Yamanaka K, Suenaga A, Hirano Y, Futatsugi N, Narumi T, Yasuoka K, Susukita R, Koishi T, Furusawa H, Kawai A, Hata M, Hoshino T, Ebisuzaki T. Molecular dynamics simulations of prion proteins – effect of Ala117 → Val mutation. *Chem-Bio Inform. J.* 2003; **3**: 1–11.
21. Liepina I, Ventura S, Czaplewski C, Liwo A. Molecular dynamics study of amyloid formation of two Abl-SH3 domain peptides. *J. Pept. Sci.* 2006; **12**: 780–789.
22. Zanuy D, Gunasekaran K, Lesk AM, Nussiov R. Computational study of the fibril organization of polyglutamine repeats reveals a common motif identified in β-helices. *J. Mol. Biol.* 2006; **358**: 330–345.
23. Zanuy D, Nussiov R. The sequence dependence of fiber organization A comparative molecular dynamics study of the islet amyloid polypeptide segments 22–27 and 22–29. *J. Mol. Biol.* 2003; **329**: 565–584.
24. Ma B, Nussinov R. Molecular dynamics simulation of alanine rich β-sheet oligomers: insight into amyloid formation. *Protein Sci.* 2002; **11**: 2335–2350.
25. Dasgupta J, Sen U, Dattagupta JK. In silico mutations and molecular dynamics studies on a winged bean chymotrypsin inhibitor protein. *Protein Eng.* 2003; **16**: 89–496.
26. Kandasamy SK, Larson RG. Molecular dynamics study of the lung surfactant peptide SP-B1–25 with DPPC monolayers: insights into interactions and peptide position and orientation. *Biophys. J.* 2005; **88**: 1577–1592.
27. Stan G, Brooks BR, Thirumalai D. Probing the "Annealing" mechanism of GroEL minichaperone using molecular dynamics simulations. *J. Mol. Biol.* 2005; **350**: 817–829.
28. Baron R, Bakowies D, van Gunsteren WF. Principles of carbopeptoid folding: a molecular dynamics simulation study. *J. Pept. Sci.* 2005; **11**: 74–84.
29. Santiveri CM, Jimenez MA, Rico M, van Gunsteren WF, Daura X. β-hairpin folding and stability: molecular dynamics simulations of designed peptides in aqueous solution. *J. Pept. Sci.* 2004; **10**: 546–565.
30. Berendsen HJC, Van der Spoel D, Van Drunen R. GROMACS: a message-passing parallel molecular dynamics implementation. *Comput. Phys. Commun.* 1995; **91**: 43–56.
31. Lindahl E, Hess B, van der Spoel D. GROMACS 30: a package for molecular simulation and trajectory analysis. *J. Mol. Model.* 2001; **7**: 306–317.
32. York DM, Wlodawer A, Pedersen LG, Darden TA. Atomic-level accuracy in simulations of large protein crystals. *Proc. Natl. Acad. Sci. U.S.A.* 1994; **91**: 8715–8718.
33. Berendsen HJC, Postma JPM, van Gunsteren NF, DiNola A, Haak IR. Molecular dynamics with coupling to an external bath. *J. Chem. Phys.* 1984; **81**: 3684–3690.
34. Hou T, Zhang W, Huang Q, Xu X. An extended aqueous solvation model based on atom-weighted solvent accessible surface areas: SAWSA v2.0 model. *J. Mol. Model.* 2005; **11**: 26–40.
35. Wang J, Wang W, Huo S, Lee M, Kollman PA. Solvation model based on weighted solvent accessible surface area. *J. Phys. Chem. B* 2001; **105**: 5055–5067.
36. Mahnam K, Moosavi-Movahedi AA, Bahrami H, Hakimelahi GH, Ataie G, Jalili S, Saboury AA, Ahmad F, Safarian S, Amanlou M. Efficient factors in protein modification : Adenosine deaminase esterification by Woodward reagent K. *J. Iran Chem. Soc.* 2008 (in press).
37. Mahnam K, Bahrami H, Moosavi-Movahedi AA, Saboury AA, Iranmanesh M, Hakimelahi GH, Soltani-Rad MN, Khalafi-Nezhad A. A theoretical investigation of mechanism of the adenosine deaminase modification: reaction of glutamate residue with woodward reagent K. *J. Theor. Comput. Chem.* 2008 (in press).
38. Chou KC, Carlacci L. Simulated annealing approach to the study of protein structures. *Protein Eng.* 1991; **4**: 661–667.
39. Villani V, Tamburro AM. Simulated annealing and molecular dynamics of an elastin-related tetrapeptide in aqueous solution. *J. Mol. Struct. (Theochem)* 1998; **431**: 205–218.
40. Rost B, Sander C. Prediction of protein structure at better than 70% accuracy. *J. Mol. Biol.* 1993; **232**: 584–599.
41. Daura X, Jaun B, Seebach D, van Gunsteren WF, Mark AE. Reversible peptide folding in solution by molecular dynamics simulation. *J. Mol. Biol.* 1998; **280**: 925–932.
42. Duan Y, Kollman PA. Pathways to a protein folding intermediate observed in a 1-microsecond simulation in aqueous solution. *Science* 1998; **282**: 740–744.
43. Schaefer M, Bartels C, Karplus M. Solution conformations and thermodynamics of structured peptides: molecular dynamics simulation with an implicit solvation model. *J. Mol. Biol.* 1998; **284**: 835–848.

44. Takano M, Yamato T, Higo J, Suyama A, Nagayama K. Molecular dynamics of a 15-residue poly (L-alanine) in water: helix formation and energetics. *J. Am. Chem. Soc.* 1999; **121**: 605–612.
45. Hummer G, Garcia AE, Garde S. Helix nucleation kinetics from molecular simulations in explicit solvent. *Proteins: Struct., Funct., Genet.* 2001; **42**: 77–84.
46. Simmerling C, Strockbine B, Roitberg AE. All-atom structure prediction and folding simulations of a stable protein. *J. Am. Chem. Soc.* 2002; **124**: 11258–11259.
47. Snow CD, Nguyen H, Pande VS, Gruebele M. Absolute comparison of simulated and experimental protein folding dynamics. *Nature* 2002; **420**: 102–106.
48. Prevost M, Ortmans I. Refolding simulations of an isolated fragment of barnase into a native-like β-hairpin: evidence for compactness and hydrogen bonding as concurrent stabilizing factors. *Proteins: Struct., Funct., Genet.* 1997; **29**: 212–227.
49. Dinner AR, Lazaridis T, Karplus M. Understanding β-hairpin formation. *Proc. Natl. Acad. Sci. U.S.A.* 1999; **96**: 9068–9073.
50. Pande VS, Rokhsar DS. Molecular dynamics simulations of unfolding and refolding of a β-hairpin fragment of protein G. *Proc. Natl. Acad. Sci. U.S.A.* 1999; **96**: 9062–9067.
51. Roccatano D, Amadei A, Di Nola A, Berendsen HJ. A molecular dynamics study of the 41–56 β-hairpin from B1 domain of protein G. *Protein Sci.* 1999; **8**: 2130–2143.
52. Bonvin AMJJ, van Gunsteren WF. β-Hairpin stability and folding: molecular dynamics studies of the first β-hairpin of tendamistat. *J. Mol. Biol.* 2000; **296**: 255–268.
53. Ferrara P, Caflisch A. Folding simulations of a threestranded antiparallel β-sheet peptide. *Proc. Natl. Acad. Sci. U.S.A.* 2000; **97**: 10780–10785.
54. Ma BY, Nussinov R. Molecular dynamics simulations of a β-hairpin fragment of protein G: balance between side-chain and backbone forces. *J. Mol. Biol.* 2000; **296**: 1091–1104.
55. Wang HW, Sung SS. Molecular dynamics simulations of three-strand β-sheet folding. *J. Am. Chem. Soc.* 2000; **122**: 1999–2009.
56. Higo J, Galzitskaya OV, Ono S, Nakamura H. Energy landscape of a β-hairpin peptide in explicit water studied by multicanonical molecular dynamics. *Chem. Phys. Lett.* 2001; **337**: 169–175.
57. Colombo G, Roccatano D, Mark AE. Folding and stability of the three-stranded β-sheet peptide Betanova: insights from molecular dynamics simulations. *Proteins: Struct., Funct., Genet.* 2002; **46**: 380–392.
58. Wu X, Wang S, Brooks BR. Direct observation of the folding and unfolding of a β-hairpin in explicit water through computer simulation. *J. Am. Chem. Soc.* 2002; **124**: 5282–5283.

DOI: 10.1002/psc